Recent Technologies for Geothermal Steam Turbines

Yoshihiro Sakai
Kenji Nakamura
Kunio Shiokawa

1. Introduction

Geothermal energy differs from fossil fuels such as oil, coal and natural gas in that it is a clean energy, having little impact on the environment and emits almost no carbon dioxide (CO_2), nitrogen oxides (NO_x) or sulfur oxides (SO_x). Fuji Electric delivered Japan's first practical geothermal power plant to the Fujita Tourist Enterprises Co. at Hakone Kowaki-en, since then has gone on to deliver more than 50 geothermal plants in Japan and around the world. Fuji Electric is counted as one of the leading manufacturers of geothermal power plants in the world.

Because geothermal steam is highly corrosive, when designing steam turbines for geothermal power generation, it is extremely important to realize and give due consideration to the corrosion of materials. For this reason, Fuji Electric has carried out continuous corrosion testing onsite at the location of geothermal power generation, and materials testing in a laboratory. The valuable data thus acquired was reflected in the turbine design in order to realize high reliability. Moreover, Fuji Electric has also actively worked to enhance the efficiency of geothermal steam turbines by applying recent blade row technology.

This paper introduces Fuji Electric's recent technologies for geothermal steam turbines.

2. Recent Materials Technology for Geothermal Steam Turbines

2.1 Corrosion testing in a modeled geothermal environment

In order to increase the reliability of geothermal steam turbines, it is important to assess the life of materials under the conditions of the geothermal environment. Fuji Electric tests the corrosiveness of geothermal steam turbine materials and evaluates their applicability to even more severe environmental conditions.

Assuming harsh conditions as the environment to which a turbine is exposed, environmental conditions were established for a concentrated corrosion test so that the long-term usage condition of a turbine could be modeled quickly. Table 1 lists the standard corrosion test environment, Table 2 lists the various corrosion tests performed in order to assess various stress conditions, and Fig. 1 shows the external appearance of the corrosion test equipment.

Table 1 Standard environment for corrosion tests

Cl	H_2S	SO_4^{2-}	pH	Temp.
10,000 ppm	300 ppm	50 ppm	3.5 to 4.0	60°C
(1.8 %, as NaCl)	(H_2S gas sealed at 0.2 L/min)	(Mixed as Na_2SO_4)		

Table 2 Contents of the corrosion test

Test	Description
Corrosion test	Immersed in a corrosive solution. Weight reduction is measured and corrosiveness is assessed.
Stress corrosion cracking (SCC) test	While applying a static stress, immersed in a corrosive solution and the time to failure is evaluated.
Corrosion fatigue test	Repeatedly applied bending load while immersed in a corrosive solution, and number of ruptures are evaluated.
Corrosion fatigue test (mean stress loading)	Static mean stress and dynamic cyclic load are applied simultaneously, and the fatigue limit is obtained.
Blunt notched compact tension (BNCT) test	Static stress is loaded, and the amount of generated SCC cracking propagation is evaluated.
Double cantilever beam (DCB) test and Stress corrosion crack propagation (K1SCC) test	Pre-cracking is formed, and the susceptibility of propagation due to the concentration of stress at the tip of the cracking is evaluated (2 types of test are performed with different shaped test specimens)

2.2 Use of new turbine materials

In existing geothermal steam turbines, 13 % Cr steel is used as the blade material and 1 % Cr steel is used as the rotor material. These materials are used widely and have a successful track record. However, we had developed and selected materials for both the blade and rotor in order to obtain even higher corrosion resistance and reliability. Table 3 lists the chemical compositions of the developed and selected

Table 3 Chemical composition of blade and rotor material that has been developed and selected

	Material	Chemical composition (%)												
		C	Si	Mn	P	S	Cr	Ni	Cu	Nb	Mo	V	W	Al
Blade material	Existing material (13 % Cr steel)	0.17 to 0.22	0.10 to 0.50	0.30 to 0.80	≦0.030	≦0.020	13.0 to 14.0	0.30 to 0.80	—	—	—	—	—	—
	Developed material (16 % Cr 4 % Ni steel)	≦0.05	0.10 to 0.35	0.30 to 0.60	≦0.025	≦0.005	15.0 to 16.0	4.2 to 5.0	3.0 to 3.7	0.20 to 0.35	—	—	—	—
Rotor material	Existing material (1 % Cr steel)	0.24 to 0.34	≦0.10	0.30 to 1.00	≦0.007	≦0.007	1.10 to 1.40	0.50 to 1.00	—	—	1.00 to 1.50	0.20 to 0.35	—	≦0.008
	Selected material (2 % Cr steel)	0.21 to 0.23	≦0.10	0.65 to 0.75	≦0.007	≦0.007	2.05 to 2.15	0.70 to 0.80	—	—	0.80 to 0.90	0.25 to 0.35	0.60 to 0.70	—
	Selected material (3.5 % Ni steel)	0.26 to 0.32	≦0.07	≦0.04	≦0.007	≦0.007	1.40 to 1.70	3.40 to 3.60	—	—	0.30 to 0.45	≦0.15	—	≦0.010

Fig.1 Corrosion cracking and corrosion fatigue test equipment

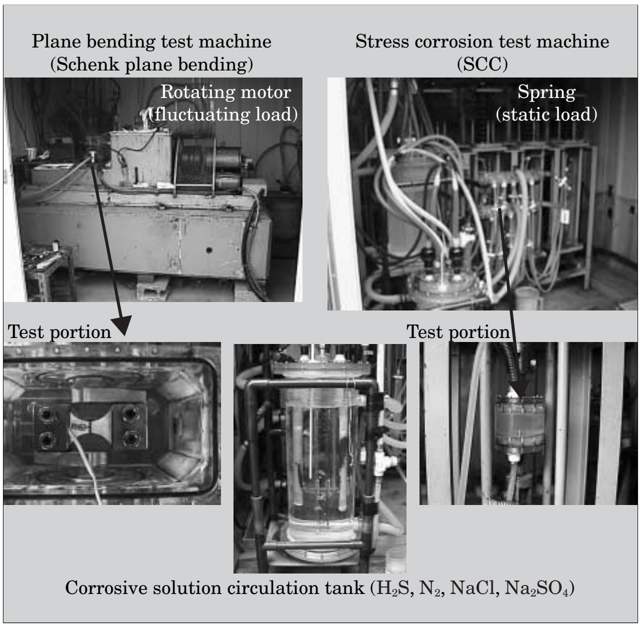

Fig.2 Fatigue limit diagram of existing and new materials

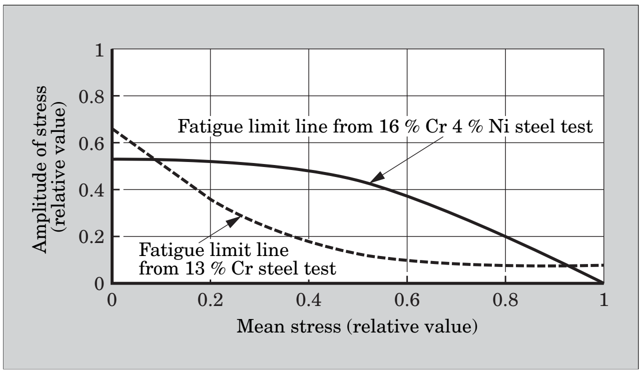

blade and rotor materials. New materials have higher chromium content than the existing materials, and this contributes to their better resistance to corrosion. The new blade materials are also heat treated appropriately in order to lower their susceptibility to corrosion and cracking.

The corrosion test described in section 2.1 was implemented for the existing blade material and for the new blade material, and the fatigue limit diagram obtained from the result of this testing is shown in Fig. 2. The results verified that under the operational stress conditions of the turbine, the new blade materials tolerated a higher stress amplitude, and exhibited higher corrosion resistance and reliability. This improvement is believed to be due to the increased chromium additive, which has the effect of suppressing the formation of corrosion pitting that has a large impact on corrosion resistance and reliability.

Figure 3 shows the results of a stress corrosion cracking propagation test (K1SCC test) that was used to evaluate the propagation of cracking at areas of

Fig.3 K1SCC test results

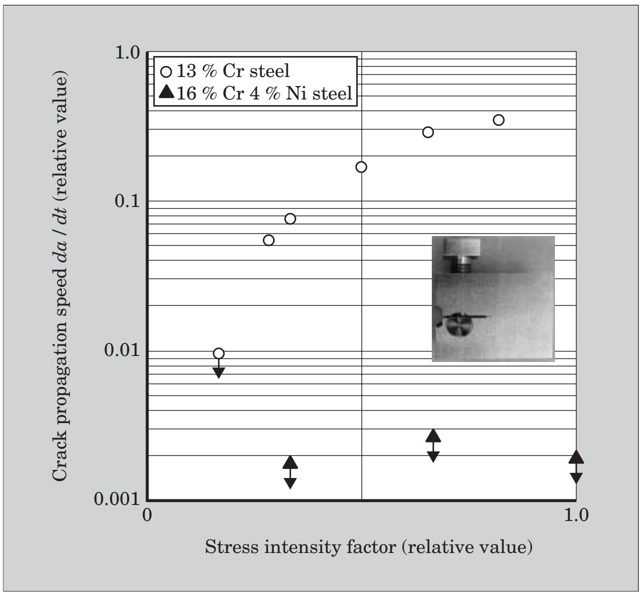

concentrated stress in both the existing material and the new blade material. The crack propagation threshold of the stress intensity factor (in units of MPa $\sqrt{m}$) was 10 MPa $\sqrt{m}$ (relative value of 0.17) for the existing blade material and 60 MPa $\sqrt{m}$ (relative value of 1.0) for the new material, thus demonstrating the superiority of this new material. On the other hand, Fig. 4 shows the results of corrosion fatigue testing

Fig.4 Results of rotor corrosion test

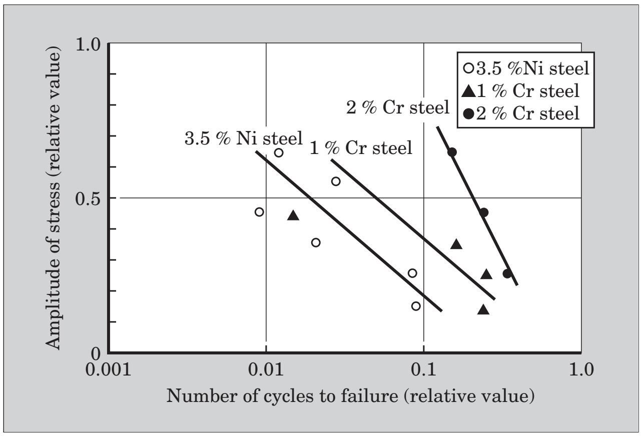

Fig.5 SCC test results (with and without shot peening)

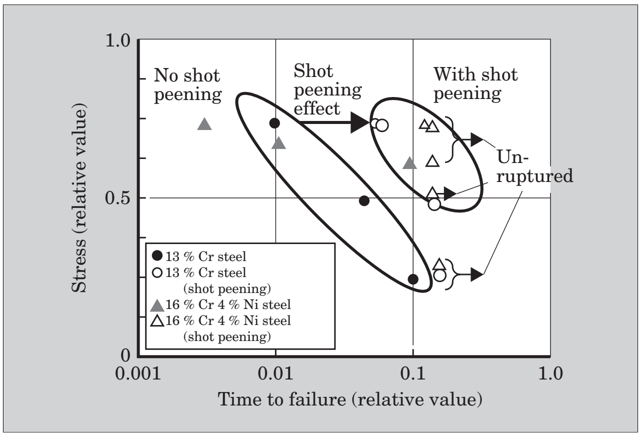

performed on the rotor material. As in the case of the blade material, it can be seen that the application of the selected material (2 % Cr steel) resulted in higher resistance to corrosion.

2.3 Shot peening technology

As described above, the application of newly developed materials was confirmed to achieve higher resistance to corrosion, but in order to support operation in an even more severe corrosive environment and under higher stress, shot peening technology is also being studied and utilized. Shot peening generates compressive residual stress by impacting a blade or rotor area in which the generated stress is severe with a steel ball having a certain amount of energy.

Stress corrosion cracking tests were performed on the shot-peened blade and rotor material, and Fig. 5 shows results that verify their longer life. It can be seen that the time to failure is at least twice as long for shot-peened material compared to material that is not shot-peened. Based on these results, Fuji Electric began using shot peening as an effective measure to increase the corrosion life of steam turbines.

2.4 Coating technology

Blade material is required to be resistant to both corrosion and to erosion. Increasing the corrosion resistance generally requires that the material's hardness be increased. However, when the hardness is increased, the stress corrosion cracking characteristics become poorer. Flame spray coating is considered to be a method potentially capable of realizing resistance to both corrosion and erosion simultaneously. Seven types of materials were selected as candidates for the flame spray coating, their hardnesses were measured, and the corrosion test described in section 2.1 and a blast erosion test were performed for each. The results are listed in Table 4. These results show that the WC-CoCr material has excellent corrosion resistance and erosion resistance as a flame spray coating material. The flame spray coating conditions were optimized for this material and the flame spray coating material and

Table 4 Results of coating test

Coating material	Stress corrosion cracking (SCC)	Fatigue	Corrosion weight reduction	Blast erosion (amount of average wear)	Hardness Hv
CoNiCrAlY+ $Al_2O_3 \cdot TiO_2$	Poor	Poor	Excellent	Good	790
WC-10Co4Cr	Excellent	Excellent	Excellent	Excellent	1,100
CoCrMo	Poor	Fair	Excellent	Good	650
Al-Zn	Poor	—	—	—	—
Stellite No. 6B spraying	—	—	Poor	Good	540
50 % Cr_3C_2-50 % NiCr	Excellent	Fair	Fair	Good	770
75 % Cr_3C_2-25 % NiCr	—	—	Fair	Good	810

— : Not tested

application method were verified to be at a level suitable for practical application to steam turbines.

2.5 Welding repair technology for the rotor

As described above, various technologies have been developed and selected in order to increase corrosion resistance. However, products that have already been delivered contain existing materials and their corrosion resistance is insufficient compared to the new products. In some geothermal steam turbines that have been in operation for a long time, corrosion has caused pitting and stress corrosion is causing cracks to appear. Accordingly, a repair technology was needed for these already-delivered products.

In the case of a rotor, stress corrosion cracking occurs at the bottom of the blade groove where the concentration of stress is highest. If cracks occur in this area, the propagation can be suppressed by shaving the area of occurrence so as to eliminate the crack. However, if the crack grows larger, it will be necessary to shave the entire blade groove. At such a time, technologies for overlay welding and for reusing the blade groove are required.

After welding conditions were selected for the plate material, welding was performed according to the dimensions of the turbine and then a mechanical property test and a corrosion test were implemented. 13 % Cr steel is used as the overlay material and the welding was implemented as multi-layer tungsten inert gas (TIG) welding.

A test specimen was sampled at the weld location, and the results of its corrosion fatigue testing are shown in Fig. 6 and the sample's overlay welding microstructure is shown in Fig. 7. The microstructure has zero defects. Excellent mechanical properties and corrosion resistance were verified for the rotor host material, and this welding repair technology was established for steam turbines.

As described above, a method has been established for assessing corrosion, which largely impacts the reliability of geothermal steam turbines, and new materials, shot peening technology, coating technology and repair technology have been developed and established. By using these materials and technologies appropriately according to the geothermal conditions and the generated stress, it is thought that higher reliability can be achieved.

In the future, Fuji Electric plans to advance the assessment and research of corrosion under geothermal conditions and intends to evaluate techniques for achieving even higher reliability and for assessing the residual life.

Fig.6 Results of corrosion fatigue test of repair welded area

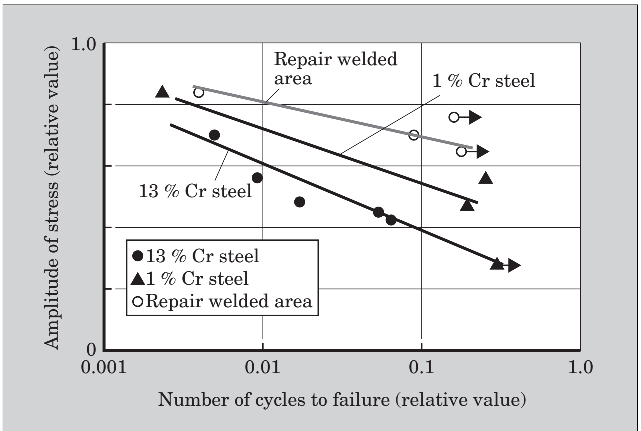

Fig.7 Microstructure of the overlay welding

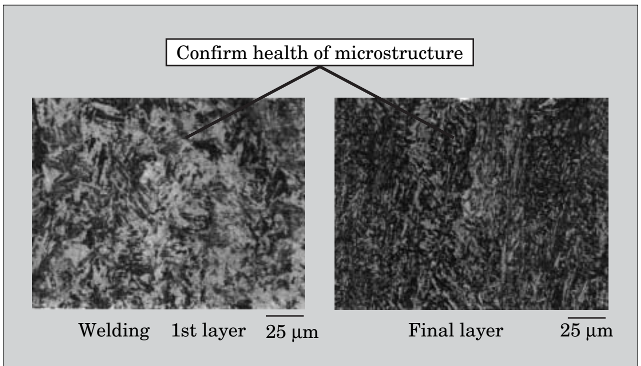

3. New technologies of Improving the Efficiency of Geothermal Steam Turbines

As a measure to improve the efficiency of geothermal steam turbines, recent technologies based on expertise acquired from the development of steam turbines for conventional thermal power generation are applied mainly to blade rows in order to realize a significant improvement in efficiency.

3.1 Advanced reaction blades (high load and high efficiency reaction blades)

Utilizing recent blade row design technology, high-efficiency reaction blades capable of maintaining high efficiency while increasing the load per stage are used in blade rows, with the exception of low-pressure blade rows, in geothermal steam turbines. For the same number of stages, the use of these reaction blades increases the efficiency by at least 1 % compared to the conventional reaction blades (see Fig. 8).

3.2 Improving the performance of low-pressure blades

Because low-pressure blades in a geothermal steam turbine account for a larger proportion of the total turbine load than in a conventional steam turbine, improving the performance of these low-pressure blades will have a greater effect on improving the performance of the total turbine than in the case of a conventional steam turbine. Originally developed for use with conventional steam turbines, a new series of low-pressure blades having much higher performance are being adjusted for use in an environment of highly corrosive geothermal steam and are being applied to actual turbines.

Below, features of this new series of low-pressure blades will be described from the perspective of their efficiency and the status of the compact-size high-efficiency low-pressure blades currently being developed will also be discussed.

Fig.8 Efficiency of conventional and advanced reaction blades

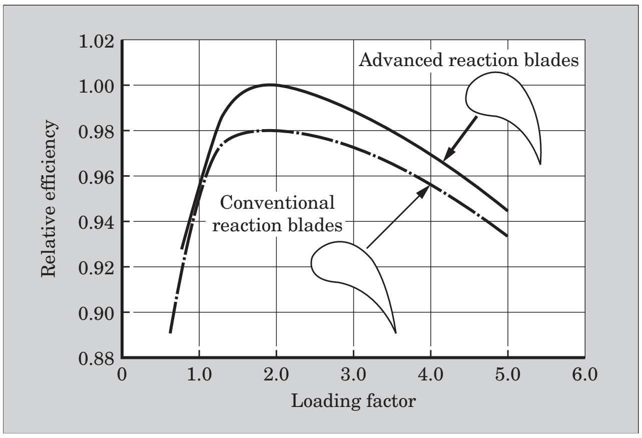

(1) Transonic profiles

Recent advances in computational fluid dynamics have made it possible to simulate accurately the flow within a blade row, and by optimizing the velocity distribution within that blade row, a low-loss profile can be realized (see Fig. 9). The new profile shape is characterized by a convergent-divergent profile (a profile designed so that the flow path widens towards the end) that is adapted for transonic flow. The results of steam wind-tunnel testing confirmed that when the outlet Mach number is large, use of the new profile shape reduces profile loss to less than 1/2 of the prior value.

(2) Lean-radial stationary blades

Using a 3-dimensional time-marching method, various profile shapes were compared while varying the flow pattern, and from the results of this comparison it could be understood that a banana-shaped stationary blade which leans toward the circumferential direction at its root and toward the radial direction at its tip, as shown in Fig. 10, was the optimal shape. By using this type of lean-radial stationary blade, flow in the vicinity of the root, where separation is likely to occur, has been improved dramatically. The results of a model turbine test confirmed that stage efficiency was improved by at least 2 % compared to the conventional stationary blades.

Fig.9 Advanced low-pressure blade analysis example and steam wind-tunnel test results

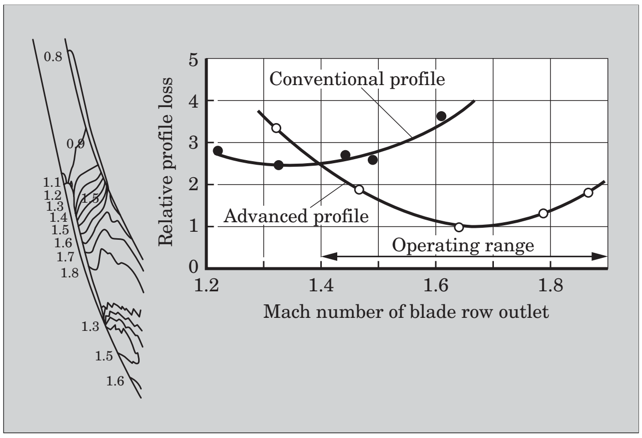

Fig.10 Results of efficiency test of lean-radial stationary blades in a model turbine

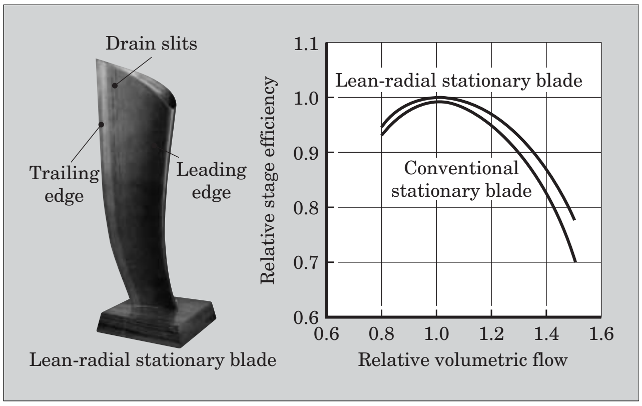

(3) Development of high efficiency, compact-size low-pressure blades

The technologies used to design the new series of low-pressure blades for conventional large steam turbines were also applied to the design of 500 mm-and-shorter low-pressure blades, and a high-efficiency compact-size low-pressure blade series that achieves dramatically higher performance is presently being developed (see Table 5).

This series is designed originally under consideration with use in geothermal steam turbines, and will also be provided the following features as well as the items adopted to enhance efficiency by using this new series of low-pressure blades.

(1) Highly reliable, rugged design for operation in a corrosive environment
(2) The blade root mounting area in all stages uses a simple inverted T-shape
(3) Redusing leakage loss from the blade tip with shroud is in all stages

Figure 11 shows the blading plan for the largest size blades (490 mm) in this series.

4. Example Applications of the Recent Technologies

Introduced below are examples of actual geothermal steam turbines to which the above-described recent technologies have been applied.

Table 5 Development of high efficiency compact-size low-pressure blades

50 Hz-use (nominal exhaust area)	60 Hz-use (nominal exhaust area)
490 mm blade (2.5 m^2)	410 mm blade (1.7 m^2)
350 mm blade (1.6 m^2)	290 mm blade (1.1 m^2)
290 mm blade (1.3 m^2)	240 mm blade (0.9 m^2)

Fig.11 Blading plan for 490 mm low-pressure blades

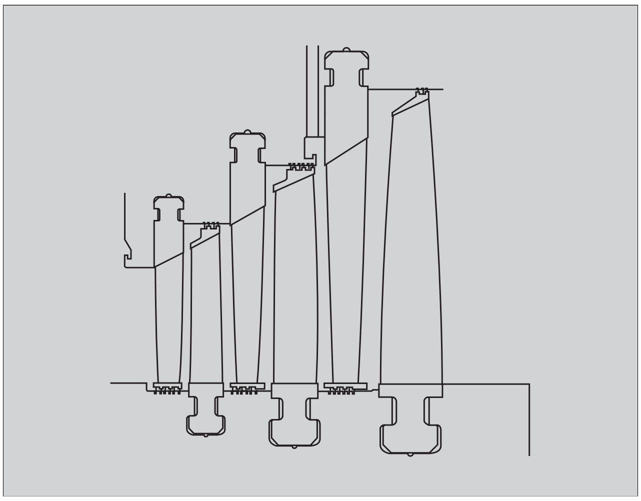

Fig.12 Cross-section of 64.7 MW geothermal steam turbine for Dixie Valley geothermal power plant

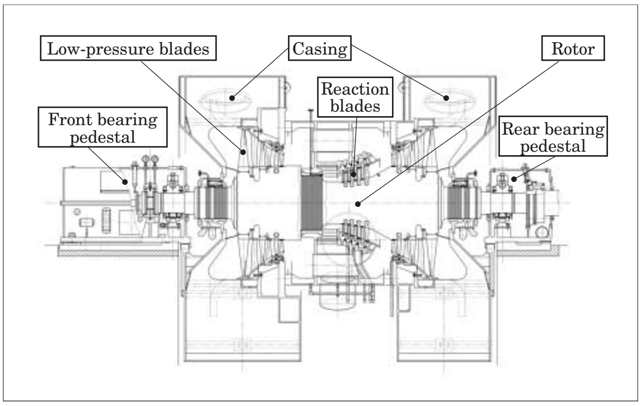

Fig.13 Cross-section of 55 MW geothermal steam turbine for Reykjanes geothermal power plant

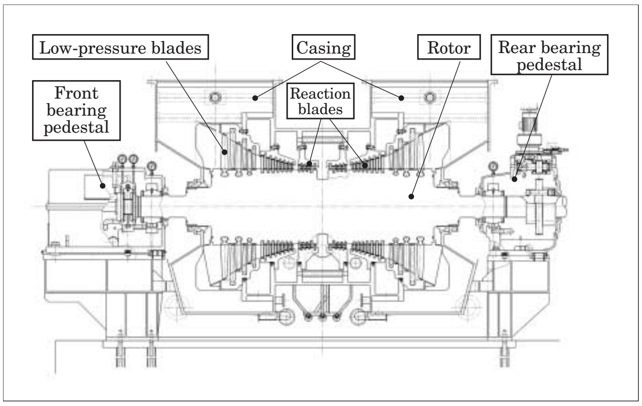

4.1 64.7 MW geothermal steam turbine for the Dixie Valley Geothermal Power Plant

Figure 12 shows a cross-sectional view of the steam turbine whose efficiency was upgraded at the Dixie Valley Geothermal Power Plant in the United States. This turbine was placed into service in 1988, and 15 years later its internal components (rotor, blades, stationary blade holder, stationary blade rings, etc.) were upgraded using the latest technology in order to increase efficiency of the turbine. The major recent technologies applied to this turbine are listed below.

(1) New blade material is used in moving blades, except in the last 2 stages
(2) New series of high-efficiency 665 mm low-pressure blades are used for the low-pressure blades (in the last 3 stages)
(3) To increase reliability, shot peening is implemented in areas of concentrated stress at the blade root and blade groove of low-pressure blades (in the last 3 stages)

The efficiency upgrade enabled this plant to increase its maximum load significantly from the previous value of 60.5 MW to 64.7 MW. After the upgrade, stable operation continued as before.

4.2 55 MW geothermal steam turbine for the Reykjanes Geothermal Power Plant

Figure 13 shows a cross-sectional view of the steam turbine currently being manufactured for the Reykjanes Geothermal Power Plant in Iceland. The characteristic features of this turbine are a high inlet steam pressure of 19 bar abs., and 2×14 blade stages, which are more stages than in a normal geothermal steam turbine.

The major recent technologies applied to this turbine are listed below.

(1) High-efficiency high-load reaction blades are used in blade rows, except for the low-pressure blades (last 3 stages)
(2) 490 mm high-efficiency compact-size low-pressure blades are used for the low-pressure blades (in the last 3 stages)
(3) 2 % Cr rotor material, which has excellent corrosion resistance, is used in the rotor
(4) New blade material is used in the moving blades at the steam inlets (main steam, admission steam)
(5) To increase reliability, shot peening is implemented in areas of concentrated stress at the blade root and blade groove of low-pressure blades (last 3 stages)

This plant is scheduled to commence operation in 2006.

5. Conclusion

Japan is a volcanic country with abundant geothermal energy resources, but at present, geothermal power generation only accounts for 0.2 % of Japan's total power generating capacity. Meanwhile, there are other countries such as the Philippines and Iceland where thermal power generation accounts for approximately 15 % of their total power generating capacity. It is hoped that geothermal power generation using domestically produced geothermal energy will continue to be developed in the future. As a leading manufacturer of geothermal power plants, Fuji Electric intends to continue to work to increase the reliability and performance of geothermal steam turbines.

References

(1) Sakai, Y. et al. Geothermal Steam Turbines with High Efficiency, High Reliability Blades. Geothermal Resources Council Transaction, Vol.24, 2000. p.521-526
(2) Sakai, Y. et al. SCC Growth Behavior of Materials for Geothermal Steam Turbines. Corrosion Engineering, Vol.53, 2004. p.175-185
(3) Sakai, Y. et al. Corrosion Resistance of Materials for Geothermal Steam Turbines. Proc. of International Conference on Power Engineering-03, Kobe, Japan. 2003.